# Reversible Formation of $[P_2PtH]_2$ Platinum(I) Complexes from *cis*-$P_2PtH_2$ Complexes, Where $P_2$ Is a Chelating Phosphine

**David J. Schwartz and Richard A. Andersen***

*Contribution from the Chemistry Department and Chemical Sciences Division of Lawrence Berkeley Laboratory, University of California, Berkeley, California 94720*

*Received July 29, 1994*[⊗]

**Abstract:** Several platinum *cis*-dihydride phosphine complexes, (diphos)$PtH_2$ [**4**, diphos = $iPr_2P(CH_2)_2PiPr_2$ (dippe); **5**, diphos = $Cy_2P(CH_2)_2PCy_2$ (dcype); and **6**, diphos = $tBu_2P(CH_2)_2PtBu_2$ (dtbpe)], have been found to be unstable in solution, reversibly losing $H_2$ and forming binuclear complexes of the general formula $[(P\text{-}P)PtH]_2$. The extent of dimerization in solution is directly related to the steric size of the phosphine ligand, larger phosphines imparting kinetic stability to the *cis*-dihydride monomers. The dimeric complexes possess terminal hydride ligands on the basis of their IR spectra; however, the room-temperature $^1H$, $^{31}P\{^1H\}$, and $^{195}Pt\{^1H\}$ NMR spectra show equivalence within the sets of H, Pt, and P nuclei, indicating that the dimers are fluxional in solution. This fluxional process can be stopped at low temperature for the (dippe) and (dcype) derivatives, **1** and **2**, but not for the (dtbpe) derivative, **3**. The complex **1** crystallizes in the orthorhombic space group $P2_12_12_1$ in a cell of dimensions $a$ = 9.245(2) Å, $b$ = 16.966(2) Å, $c$ = 22.690(6) Å, and $Z$ = 4. The structure shows square planar geometry about each Pt(I) center, the coordination sphere being composed of one bidentate phosphine ligand, a terminal hydride, and a direct, unbridged bond to the other Pt center. The angle between the two square planes is 93.2(1)°, and the Pt−Pt distance is 2.5777(5) Å. The complex **3** crystallizes as a toluene solvate in the triclinic space group $P\bar{1}$ with $a$ = 11.552(3) Å, $b$ = 13.123(3) Å, $c$ = 17.694(4) Å, $\alpha$ = 81.20(2)°, $\beta$ = 89.20(2)°, $\gamma$ = 66.55(2)°, and $Z$ = 2. The structure is similar to that of **1**; however, there are several distortions resulting from steric crowding caused by the larger *tert*-butyl groups (Pt−Pt distance = 2.6094(6) Å). The spectral and structural details, the solution properties, and the nature of the fluxional process are discussed.

## Introduction

Monohydrides of platinum(II) with monodentate phosphine ligands, for example *trans*-$Pt(H)(Cl)(PEt_3)_2$, were first prepared by Chatt in 1957.[1a,b] The *trans*-dihydrides are less stable, and no isolated compounds were described until 1974 when Shaw used sterically bulky phosphines in order to prevent decomposition.[1c] Shaw also showed that the *cis*-dihydrides are stable toward loss of dihydrogen only when chelating bidentate phosphines with sterically bulky substituents are used.[1d,2]

Consistent with this latter concept, in the course of preparing *cis*-$(P\text{-}P)PtH_2$ complexes of various phosphines, Otsuka and co-workers[3] found that only the derivatives containing sterically bulky phosphines were stable in solution. Solutions of the derivatives containing smaller phosphines gradually darkened in color, and the intensity of the hydride resonance in the $^1H$ NMR spectrum, as well as the Pt−H stretch in the infrared spectrum, diminished over time. Otsuka *et al.* suggested that for the $(P\text{-}P)PtH_2$ derivatives containing sterically smaller phosphines, reversible loss of dihydrogen was occurring to give $(P_2Pt)_2$ dimers in solution. This postulate was made on the basis of the above observations and the fact that reduction of (dtbpp)-$PtCl_2$ (dtbpp = $(tBu)_2P(CH_2)_3P(tBu)_2$) in tetrahydrofuran yields only the hydride-free compound $Pt_2(dtbpp)_2$. This reddish-orange Pt(0) dimer is controversial since some chemical reactions imply the presence of Pt−H bonds, suggesting that perhaps more than one species is present in solution.[3a]

Similarly, $(Cy_2P(CH_2)_nPCy_2)PtH_2$ ($n$ = 2, dcype; $n$ = 3, dcypp) have also been reported to be unstable in solution.[4a] The monomers lose dihydrogen in solution and generate a species that was identified as a dimer, $[(P\text{-}P)PtH]_2$, by $^1H$ and $^{31}P\{^1H\}$ NMR spectroscopy. This deduction was questioned by Pidcock and co-workers[4b] since they showed that warming a solution of $(dppe)PtH_2$ (dppe = $Ph_2P(CH_2)_2PPh_2$), formed at low temperature, to room temperature yields the dimer $[(dppe)PtH]_2$, whose $^1H$ and $^{31}P$ NMR spectra are very different from those of the (dcype) and (dcypp) derivatives in ref 4a. The latter complexes give NMR spectra that are similar to those that have been observed for cationic complexes of the type $[(P\text{-}P)_2Pt_2H_3][X]$; the proton source is presumably $H_2O$, so the anion is $(OH^-)$.[4b] The fluxional cation, $[(P\text{-}P)_2Pt_2H_3][X]$, with either one or two bridging hydrides in the solid state, is a pervasive structural feature in platinum hydride chemistry.[5] The hydrides in

* Address correspondence to this author at Chemistry Department. University of California, Berkeley, CA 94720.

⊗ Abstract published in *Advance ACS Abstracts*, March 1, 1995.

(1) (a) Chatt, J.; Duncanson, L. A.; Shaw, B. L. *Proc. Chem. Soc., London* **1957**, 343. (b) Chatt, J.; Shaw, B. L. *J. Chem. Soc., London* **1962**, 5075. (c) Shaw, B. L.; Uttley, M. F. *J. Chem. Soc., Chem. Commun.* **1974**, 918. (d) Moulton, C. J.; Shaw, B. L. *Ibid.* **1976**, 365.

(2) (a) *Transition Metal Complexes of Phosphorus, Arsenic, and Antimony Ligands*; McAuliffe, C. A., Ed.; John Wiley: New York, 1973. (b) McAuliffe, C. A.; Levason, W. *Phosphine, Arsine, and Stibine Complexes of the Transition Elements*; Elsevier: New York, 1979.

(3) (a) Yoshida, T.; Yamagata, T.; Tulip, T. H.; Ibers, J. A.; Otsuka, S. *J. Am. Chem. Soc.* **1978**, *100*, 2063. (b) Tulip, T. H.; Yamagata, T.; Yoshida, Y.; Wilson, R. D.; Ibers, J. A.; Otsuka, S. *Inorg. Chem.* **1979**, *18*, 2239.

(4) (a) Clark, H. C.; Hampden-Smith, M. J. *J. Am. Chem. Soc.* **1986**, *108*, 3829. (b) Carmichael, D.; Hitchcock, P. B.; Nixon, J. F.; Pidcock, A. *J. Chem. Soc., Chem. Commun.* **1988**, 1554. (c) Serivanti, A.; Campustrini, R.; Caruran, G. *Inorg. Chim. Acta* **1988**, *142*, 187.

(5) (a) Bracher, G.; Grove, D. M.; Pregosin, P. S.; Venanzi, L. M. *Angew. Chem., Int. Ed. Engl.* **1979**, *18*, 155. (b) Carmona, D.; Thouvenot, R.; Venanzi, L. M.; Bachechi, F.; Zambonelli, L. *J. Organomet. Chem.* **1983**, *250*, 589. (c) Bachechi, F.; Bracher, G.; Grove, D.; Kellenberger, D. M.; Pregosin, P. S.; Venanzi, L. M.; Zambonelli, L. *Inorg. Chem.* **1983**, *22*, 1031. (d) Bachechi, F. *Acta Crystallogr.* **1993**, *C49*, 460. (e) Knobler, C. B.; Kaesz, H. D.; Minghetti, G.; Bandini, A. L.; Banditelli, G.; Bonati, F. *Inorg. Chem.* **1983**, *22*, 2324. (f) Chiang, M. Y.; Bau, R.; Minghetti, G.; Bandini, A. L.; Banditelli, G.; Koetzle, T. F. *Ibid.* **1984**, *23*, 122. (g) Aime, S.; Gobetto, R.; Bandini, A. L.; Banditelli, G.; Minghetti, G. *Ibid.* **1991**, *30*, 316. (h) Paonessa, R. S.; Trogler, W. C. *Ibid.* **1983**, *22*, 1038.

0002-7863/95/1517-4014$09.00/0 

(dcypp)$PtH_2$ are also fluxional; they undergo mutual exchange on the NMR time scale, and it has been suggested that $\eta^2$-hydrogen complexes are involved.[4a,c]

This novel suggestion was the origin of our studies since we though that it might be possible to displace the hypothetical dihydrogen ligand with $(Me_5C_5)_2Yb$. As part of an endeavor to use (P-P)Pt and *cis*-(P-P)$PtH_2$ complexes as ligands toward $(Me_5C_5)_2Yb$,[6] we prepared various dihydrides with chelating bidentate phosphine ligands. We observed that these compounds lose dihydrogen to a variable extent, depending upon the substituents on phosphorus, and that the resulting dimers, [(P-P)Pt$H]_2$, are fluxional in solution. These dimers have never been studied in detail, and no crystal structures of these neutral dimeric platinum hydrides have been reported, though they are generally written as if they contain bridging hydride ligands,[4] analogous to [(dcypp)Ni($\mu$-H)$]_2$.[7a,b] Recently, the related palladium hydride dimer, [(dippp)Pd($\mu$-H)$]_2$, has been described.[7c] In the solid state, the hydride ligands bridge the two palladium centers in an unsymmetrical manner, and the $P_2Pd$ planes are twisted relative to each other by 20°, compared to a twist angle in the nickel dimer of 63°. In solution both molecules are fluxional, with equivalency within the sets of hydride and phosphorus nuclei.

## Results

**Syntheses.** Stirring a THF solution of $[(Me_2CH)_2P(CH_2)_2P(CHMe_2)_2]PtCl_2$, (dippe)$PtCl_2$, with sodium amalgam at room temperature under 1 atm of hydrogen for 1 day gave [(dippe)Pt$H]_2$ (**1**) as the sole product, isolated in 62% yield. This result was unexpected as the synthetic method is identical (except for the identity of the phosphine) to that used by Otsuka to synthesize (dtbpe)$PtH_2$.[3a] The dimer **1** is light brown in color, soluble in aliphatic hydrocarbons, and volatile enough to give a molecular ion in the mass spectrum. The dimeric nature of **1** is clear from the $^{31}P\{^1H\}$ NMR spectrum, in which two different $^{195}Pt-^{31}P$ coupling constants are observed. The solid state infrared spectrum shows two strong bands at 1939 and 1926 $cm^{-1}$, indicating the presence of terminal hydride ligands. The $^1H$-coupled $^{195}Pt$ INEPT NMR spectrum (see supplementary material) shows that there are two hydrides per dimer. The hydride region of the $^1H$ NMR spectrum of **1** shows an apparent "quintet of quintets",[3b,5e] indicating equivalency on the NMR time scale within the sets of four phosphorus, two platinum, and two hydride nuclei, at 25 °C.

A similar synthetic procedure using the cyclohexylphosphine derivative, (dcype)$PtCl_2$, yields the known monomer (dcype)Pt$H_2$ (**5**)[4a] in 85% yield after crystallization from THF, as colorless crystals. Inspection of the $^{31}P\{^1H\}$ NMR spectrum of the crude reaction mixture in $C_6D_6$ showed that it contained a *ca.* 9:1 ratio of **5** and a material shown to be the dimer [(dcype)Pt$H]_2$ (**2**). This ratio is unchanged indefinitely under nitrogen at room temperature and is also unchanged after prolonged heating at 90 °C in a closed system. However, heating a sample of **5** in toluene at reflux for 16 h under a slow purge of nitrogen (*i.e.*, in an *open* system) gives **2** as a yellow powder in 58% isolated yield. The NMR data for **2** are similar to those of **1**. The solid state infrared spectrum shows two features at 1965 and 1937 $cm^{-1}$, due to terminal Pt−H stretches.

As mentioned in the Introduction, conversion of **5** to **2** in solution has been reported in the literature.[4a] In contrast to our findings, these authors reported that room-temperature solutions of **5** gave complete conversion to **2** within 1 h. In addition, Pidcock and co-workers have suggested that the species identified by Clark and Hampden-Smith as "[(dcype)Pt($\mu$-H)$]_2$" was actually $[(dcype)_2Pt_2H_3]^+$, where the anion is presumably hydroxide. We have found that adding several drops of water to a benzene solution of **5** results in clean conversion to $[(dcype)_2Pt_2H_3]^+[OH]^-$. The NMR values of this cationic complex (see later discussion) show that this is indeed the complex that Clark and Hampden-Smith identified as **2**; our results confirm the suggestion made by Pidcock *et al.*[4b]

**Table 1.** $^1H$ and $^{31}P\{^1H\}$ NMR Data for the Dimers **1**−**3** (25 °C, $C_6D_6$) and [(dippe)Pt$H]_2$

| | $\delta$ (Pt−H), ppm | $^2J_{PH}$, Hz | $^1J_{PtH}$, Hz | $\delta$ (P), ppm | $^{1,2}J_{PtP}$, Hz | $^3J_{PP}$,[a] Hz |
|---|---|---|---|---|---|---|
| **1** | 0.49 | 40 | 516 | 105.5 | 2210, 410 | 45 |
| **2** | 0.49 | 40 | 512 | 92.8 | 2180, 420 | 44 |
| **3** | 0.05 | 42 | 570 | 119.9 | 3112, 362 | 47 |
| [(dppe)Pt$H]_2$[b] | 0.30 | 42 | 564 | 70.9 | 2201, 388 | 44 |

[a] This coupling is expressed only in the $Pt/^{195}Pt$ and $^{195}Pt/^{195}Pt$ subspectra. [b] Values taken from ref 4b and measured in THF-$d_8$.

A benzene solution of (dtbpe)$PtH_2$ (**6**), prepared using Otsuka's method,[3a] is stable indefinitely at room temperature under nitrogen, as was found for **5**. In contrast to **5**, no evidence of a dimeric complex is seen in the $^1H$ and $^{31}P\{^1H\}$ NMR spectra of the crude reaction mixture. Otsuka and co-workers reported that **6** is stable in solution up to temperatures of 100 °C. We found that this is indeed true for a toluene solution of **6** in a closed system. However, analogous to **5**, heating a toluene solution of **6** at 90 °C for 16 h under a slow purge of nitrogen gives a reddish-brown solution from which [(dtbpe)Pt$H]_2$ (**3**) can be isolated in 73% yield as dark orange crystals. This dimer also shows two terminal Pt−H stretching frequencies in the infrared spectrum at 1975 and 1951 $cm^{-1}$. The dimer **3** is stable indefinitely in benzene under nitrogen at room temperature and has $^1H$ and $^{31}P\{^1H\}$ NMR spectra similar to those of **1** and **2** (Table 1).

**Monomer/Dimer Equilibrium.** Benzene solutions of all of the dimers, **1**−**3**, are stable at room temperature under a nitrogen atmosphere. However, when the nitrogen is replaced by hydrogen gas (1 atm), quantitative conversion to the *cis*-dihydride monomers occurs within 24 h for all three samples; conversion was followed by $^{31}P\{^1H\}$ NMR spectroscopy. The (dippe)$PtH_2$ monomer (**4**) was not isolated as it is only stable under an atmosphere of hydrogen gas; its identity was deduced by the similarity of its $^1H$ and $^{31}P\{^1H\}$ NMR spectral values to those of **5** and **6** (Table 2).

Solutions of **5** and **6** (converted from **2** and **3**) were then stable indefinitely when the hydrogen was replaced by nitrogen. In contrast, the sample of **4** slowly reverted to **1** when the hydrogen atmosphere was replaced by nitrogen; the sample consisted of a *ca.* 2:1 ratio of **1**:**4** after 100 h at room temperature under nitrogen. Interconversion of **1** and **4** was found to be facile, depending upon whether $N_2$ or $H_2$ was present over the solution (eq 1). This interconversion is clean, with no byproducts observed in the $^{31}P\{^1H\}$ spectrum, indicating that eq 1 is a reversible chemical equilibrium.

$$\underset{\mathbf{4}}{2(\text{dippe})PtH_2} \underset{(+H_2)}{\overset{1\text{ atm }H_2}{\rightleftharpoons}} \underset{\mathbf{1}}{[(\text{dippe})PtH]_2} \qquad (1)$$

**Solid State Structures of 1 and 3.** The ORTEP diagrams of **1** and **3** are shown in Figures 1 and 2, respectively. The crystallographic data (Table 3), positional parameters (Tables 4 and 5), and selected bond lengths and angles (Table 6) are

(6) These studies will be reported later.

(7) (a) Jonas, K.; Wilke, G. *Angew. Chem., Int. Ed. Engl.* **1970**, *9*, 312. (b) Barnett, B. L.; Kruger, C.; Tsay, Y.-H.; Summerville, R. H.; Hoffmann, R. *Chem. Ber.* **1977**, *110*, 3900. (c) Fryzuk, M, D.; Lloyd, B. R.; Clentsmith, G. K. B.; Rettig, S. J. *J. Am. Chem. Soc.* **1994**, *116*, 3804.

**Table 2.** $^1H$ and $^{31}P\{^1H\}$ NMR Data for the Monomers **4**–**6** (25 °C, $C_6D_6$)

| | δ (Pt–H), ppm | $^2J_{P\text{-}trans\text{-}H}$, Hz | $^2J_{P\text{-}cis\text{-}H}$, Hz | $^1J_{PtH}$, Hz | δ (P), ppm | $^1J_{PtP}$, Hz |
|---|---|---|---|---|---|---|
| **4**[a] | 0.46 | 179 | 16 | 1097 | 87.9 | 1829 |
| **5** | 0.56 | 179 | 16 | 1100 | 78.2 | 1822 |
| **6** | −0.54 | 180 | 16 | 1096 | 107.8 | 1872 |

[a] Not isolated, see text.

given. The hydride ligands could not be located, but their positions are inferred from the square planar geometry about each platinum center. Qualitatively, both structures contain two square planar platinum centers, the coordination sphere of each consisting of two phosphorus atoms, one hydride, and the other platinum atom; the idealized symmetry is $C_2$. Formally, both metal centers are in the +I oxidation state and a metal–metal bond is present, accounting for the observed diamagnetism. Dimeric platinum hydride complexes possessing an unbridged Pt–Pt bond have not been structurally characterized before.

Considering first the structure of **1**, the Pt–P bond distances in **1** are in the expected range.[3a,8] The distances for the pair of phosphorus atoms *trans* to the hydrides (Pt(1)–P(1), 2.257(3) Å; Pt(2)–P(3), 2.254(3) Å) are identical within experimental error to the analogous distances for the pair *trans* to the other platinum atom (Pt(1)–P(2), 2.242(3) Å, Pt(2)–P(4), 2.244(3) Å), indicating that the terminal Pt–H bond and the Pt–Pt bond have similar *trans* influences. The Pt(1)–Pt(2) separation of 2.5777(5) Å for **1** is consistent with a direct, unbridged Pt(I)–Pt(I) bond and is within the range found in the four Pt(I) dimers containing unbridged Pt–Pt bonds that have been crystallographically characterized (2.53–2.63 Å).[9] These distances are shorter than expected, considering that the covalent radius of Pt(0) is 1.38 Å[10] and that of Pt(II) is 1.31 Å.[11] Many Pt(I) dimers with bridging ligands are known, and they have been reviewed.[12]

The P–Pt–Pt angles of 102.1° for P(3)–Pt(2)–Pt(1), 100.5° for P(1)–Pt(1)–Pt(2), 168.6° for P(2)–Pt(1)–Pt(2), and 167.4° for P(4)–Pt(2)–Pt(1), none of which deviate from the idealized square planar values (90° for the first pair, 180° for the latter pair) by more than 13°, are also consistent with the presence of two terminal hydrides. The analogous values for $[(PCy_3)(SiEt_3)Pt(\mu\text{-}H)]_2$ are 123–134°.[13] This lack of deviation from idealized square planar values indicates that steric interactions between isopropyl groups of the phosphines are negligible, as such interactions would result in an opening of the P(3)–Pt(2)–Pt(1) and P(1)–Pt(1)–Pt(2) angles from the idealized value of 90°. Examination of the isopropyl groups on P(1) and P(3) shows that these steric interactions are minimized by the orientation of the alkyl groups; the methine hydrogen atoms on C(11) and C(30) point toward, while the larger methyl groups point away from, each other.

The dihedral angle between the planes defined by P(1)–Pt(1)–P(2)/P(3)–Pt(2)–P(4) is 93°. The analogous angle in

**Table 3.** Crystallographic Data for $[(dippe)PtH]_2$ (**1**) and $[(dtbpe)PtH]_2$ (**3**)

| | **1** | **3** |
|---|---|---|
| chemical formula | $Pt_2P_4C_{28}H_{66}$ | $Pt_2P_4C_{36}H_{82}$ |
| molecular weight | 916.92 | 1029.13 |
| crystal size, mm | 0.48 × 0.45 × 0.18 | 0.50 × 0.38 × 0.23 |
| space group | $P2_12_12_1$ | $P\bar{1}$ |
| $a$, Å | 9.245(2) | 11.552(3) |
| $b$, Å | 16.966(2) | 13.123(3) |
| $c$, Å | 22.690(6) | 17.694(4) |
| α, deg | 90 | 81.20(2) |
| β, deg | 90 | 89.20(2) |
| γ, deg | 90 | 66.55(2) |
| $V$, Å$^3$ | 3559(1) | 243(1) |
| $Z$ | 4 | 2 |
| $d$ (calcd), g cm$^{-3}$ | 1.713 | 1.407 |
| $\mu$ (calcd), cm$^{-1}$ | 81.4 | 59.6 |
| $T$, °C | −95 | −88 |
| reflections measured | $+h,+k,+l$ | $+h,\pm k,\pm l$ |
| 2φ range, deg | 3–55 | 3–50 |
| reflections collected | 4630 | 8658 |
| max corrn for crystal decay | 1.4% on $F$ | 2.1% on $F$ |
| absorption corrn[a] | $T_{max} = 1.31$, $T_{min} = 0.759$ | $T_{max} = 0.998$, $T_{min} = 0.677$ |
| atoms in least squares | 34 | 59 |
| unique reflections | 4567 | 8529 |
| reflections with $F^2 > 3\sigma(F^2)$ | 3646 | 6398 |
| $p$ factor | 0.04 | 0.04 |
| parameters | 308 | 403 |
| $R$[b] | 0.0344 | 0.0533 |
| $R_w$ | 0.0371 | 0.0675 |
| $R_{all}$ | 0.0529 | 0.0753 |
| GOF | 1.070 | 2.212 |
| difference Fourier, e$^-$ Å$^{-3}$ | +1.4, −0.37 | +3.2, −0.29 |

[a] The program DIFABS[22] was used for the absorption correction for **1**; an empirical absorption correction based on the azimuthal scans was done for **3**. [b] The definitions for $R$ and $R_w$ are as follows: $R = \sum||F_o| - |F_c||/\sum|F_o|$ and $R_w = \sqrt{\sum w(|F_o| - |F_c|)^2/\sum wF_o^2}$.

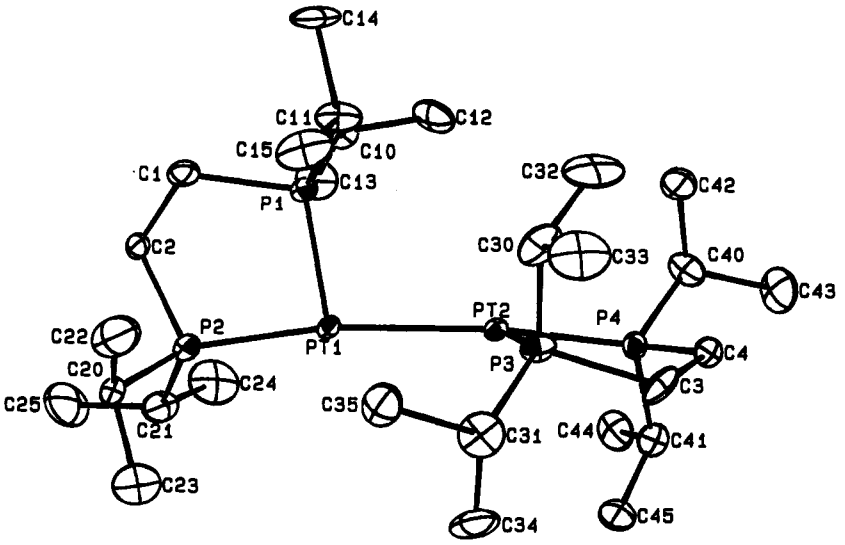


**Figure 1.** ORTEP diagram of $[(dippe)PtH]_2$ (**1**) with 50% probability ellipsoids.

**Table 4.** Atomic Coordinates and $B$ Values (Å$^2$) for the Non-Hydrogen Atoms of Compound **1**[a]

| atom | $x$ | $y$ | $z$ | $B_{equiv}$[b] |
|---|---|---|---|---|
| PT1 | 0.4034(1) | 0.10695(1) | 0.27179(1) | 1.015(6) |
| PT2 | 0.42467(1) | 0.09281(1) | 0.15894(1) | 0.975(6) |
| P1 | 0.4308(4) | −0.0199(2) | 0.2998(1) | 1.26(5) |
| P2 | 0.4113(4) | 0.1415(2) | 0.3671(1) | 1.80(6) |
| P3 | 0.1906(3) | 0.0888(2) | 0.1312(1) | 1.58(6) |
| P4 | 0.4850(3) | 0.0976(2) | 0.0632(1) | 1.28(5) |
| C1 | 0.420(2) | −0.0234(6) | 0.3820(5) | 1.9(2) |
| C2 | 0.468(2) | 0.0538(7) | 0.4111(5) | 2.3(3) |
| C3 | 0.179(1) | 0.1098(8) | 0.0509(5) | 2.2(2) |
| C4 | 0.318(1) | 0.0851(7) | 0.0182(5) | 1.8(2) |
| C10 | 0.605(1) | −0.712(7) | 0.2834(5) | 1.9(2) |
| C11 | 0.296(1) | −0.0922(7) | 0.2773(6) | 2.1(2) |
| C12 | 0.615(1) | −0.0951(7) | 0.2193(6) | 2.7(3) |
| C13 | 0.726(2) | −0.0182(9) | 0.3002(6) | 3.1(3) |
| C14 | 0.323(2) | −0.1766(7) | 0.2999(6) | 2.9(3) |
| C15 | 0.143(2) | −0.0654(9) | 0.2930(7) | 3.1(3) |
| C20 | 0.246(2) | 0.1762(7) | 0.4047(5) | 2.1(3) |
| C21 | 0.550(2) | 0.2142(7) | 0.3876(5) | 3.3(3) |
| C22 | 0.125(2) | 0.1161(9) | 0.3992(6) | 4.2(3) |
| C23 | 0.197(2) | 0.2541(9) | 0.3799(7) | 4.0(4) |
| C24 | 0.696(2) | 0.197(1) | 0.3583(7) | 4.0(3) |
| C25 | 0.568(2) | 0.2245(9) | 0.4560(6) | 5.2(4) |
| C30 | 0.099(2) | −0.0067(8) | 0.1387(5) | 2.6(3) |
| C31 | 0.060(1) | 0.1608(8) | 0.1607(6) | 2.5(3) |
| C32 | 0.186(2) | −0.0730(8) | 0.1097(7) | 3.8(3) |
| C33 | −0.057(2) | −0.0087(9) | 0.1160(7) | 3.6(3) |
| C34 | 0.121(2) | 0.2464(8) | 0.1580(6) | 3.2(3) |
| C35 | 0.012(2) | 0.1404(9) | 0.2240(6) | 2.9(3) |
| C40 | 0.612(1) | 0.0264(7) | 0.0299(5) | 2.2(2) |
| C41 | 0.561(2) | 0.1930(7) | 0.0397(5) | 2.3(3) |
| C42 | 0.573(2) | −0.0577(7) | 0.0446(5) | 3.1(3) |
| C43 | 0.634(2) | 0.0386(9) | −0.0365(6) | 3.4(3) |
| C44 | 0.714(2) | 0.2018(9) | 0.0630(5) | 3.0(3) |
| C45 | 0.463(2) | 0.2606(7) | 0.0604(5) | 2.6(3) |

[a] Numbers in parentheses give estimated standard deviations. [b] Equivalent isotropic thermal parameters are calculated as $^4/_3$ [$\alpha^2\beta_{11} + b^2\beta_{22} + c^2\beta_{33} + ab(\cos\gamma)\beta_{12} + ac(\cos\beta)\beta_{13} + bc(\cos\alpha)\beta_{23}$].

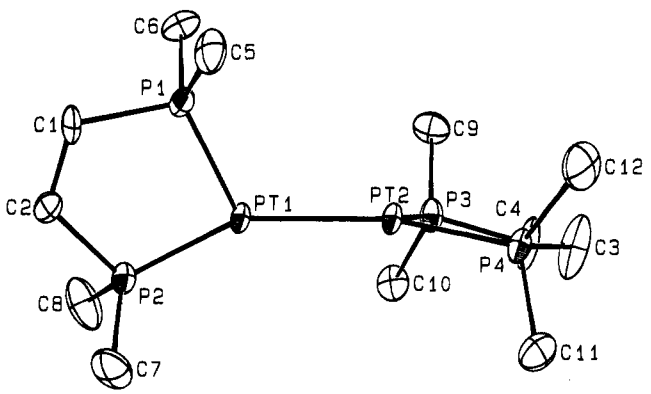


**Figure 2.** ORTEP diagram of [(dtbpe)PtH]$_2$ (**3**) with 50% probability ellipsoids. For clarity, the disordered methyl groups and the toluene solvate are not shown. No hydrogen atoms were included in the model (see Experimental Section for details).

[(dtbpp)Pt]$_2$ is 82°.[3a] For the latter structure, in which the P−Pt−Pt angles are *ca.* 128°, a 90° dihedral angle would minimize steric interactions between the large *tert*-butyl groups on the phosphine ligands, and this is probably the reason for the 82° angle. However, since the P(1)−Pt(1)−Pt(2) and P(3)−Pt(2)−Pt(1) angles in **1** are *ca.* 101°, such steric interactions would be minimized if this dihedral angle were 180° (there are actually two 180° orientations, the orientation being discussed has the hydrides *trans* to each other, relative to the Pt−Pt vector, Figure 3). This geometry places all of the alkyl groups on the phosphine ligands near hydrides, as opposed to near other alkyl groups, and minimizes the steric interactions discussed in the previous paragraph. The dihedral angle in the nickel analogue, [(dcypp)Ni($\mu$-H)]$_2$,[7b] is 63°, and this was rationalized on the basis of a steric argument. In the palladium analogue, [(dippp)-Pd($\mu$-H)]$_2$,[7c] it is 20°, and this was rationalized by assuming that the larger size of Pd results in minimal steric interactions between the isopropyl groups on opposite ends of the dimer.

(8) Orpen, A. G.; Brammer, L.; Allen, F. H.; Kennard, O.; Watson, D. G.; Taylor, R. *J. Chem. Soc., Dalton Trans.* **1989**, 51. This article lists Pt−P distances for a variety of compounds in various oxidation states and coordination numbers.

**Table 5.** Atomic Coordinates and $B$ Values (Å$^2$) for the Atoms of Compound **3**

| atom | $x$ | $y$ | $z$ | $B_{equiv}$ |
|---|---|---|---|---|
| PT1 | 0.09551(1) | 0.23233(1) | 0.30281(1) | 1.594(9) |
| PT2 | 0.28116(1) | 0.05574(1) | 0.26754(1) | 1.610(9) |
| P1 | 0.1074(3) | 0.4004(2) | 0.2611(2) | 2.00(7) |
| P2 | −0.0631(3) | 0.3169(2) | 0.3766(2) | 1.82(6) |
| P3 | 0.2296(3) | −0.0261(3) | 0.1760(2) | 2.04(7) |
| P4 | 0.4687(3) | −0.0937(2) | 0.2913(2) | 1.82(6) |
| C1 | −0.015(1) | 0.506(1) | 0.3114(9) | 3.7(3) |
| C2 | −0.080(1) | 0.465(1) | 0.3688(9) | 4.3(4) |
| C3 | 0.477(1) | −0.193(1) | 0.2264(9) | 4.6(3) |
| C4 | 0.357(1) | −0.170(1) | 0.1806(9) | 4.2(4) |
| C5 | 0.259(1) | 0.414(1) | 0.2892(8) | 2.9(3) |
| C6 | 0.063(1) | 0.463(1) | 0.1566(8) | 3.0(3) |
| C7 | −0.028(1) | 0.264(1) | 0.4826(8) | 3.7(4) |
| C8 | −0.230(1) | 0.331(1) | 0.3508(9) | 4.7(4) |
| C9 | 0.223(1) | 0.039(1) | 0.0720(8) | 3.2(3) |
| C10 | 0.087(1) | −0.065(1) | 0.1930(8) | 2.9(3) |
| C11 | 0.487(1) | −0.179(1) | 0.3880(9) | 3.8(4) |
| C12 | 0.618(1) | −0.070(1) | 0.270(1) | 4.6(4) |
| C13 | 0.371(1) | 0.334(1) | 0.249(1) | 5.6(5) |
| C14 | 0.253(1) | 0.537(1) | 0.269(1) | 4.1(4) |
| C15 | 0.274(2) | 0.379(1) | 0.376(1) | 5.7(4) |
| C16 | 0.026(2) | 0.592(1) | 0.136(1) | 5.2(5) |
| C17 | 0.174(2) | 0.404(1) | 0.1072(9) | 5.3(5) |
| C18 | −0.050(1) | 0.433(1) | 0.135(1) | 6.3(5) |
| C19 | −0.121(2) | 0.335(1) | 0.5338(9) | 5.0(4) |
| C20 | −0.051(2) | 0.144(2) | 0.497(1) | 3.8(5)[a] |
| C20′ | 0.045(4) | 0.145(3) | 0.511(3) | 5(1)[a] |
| C21 | 0.114(2) | 0.222(2) | 0.499(1) | 3.7(5)[a] |
| C21′ | 0.084(3) | 0.321(3) | 0.498(2) | 3.3(7)[a] |
| C22 | −0.332(1) | 0.391(1) | 0.401(1) | 4.7(4) |
| C23 | −0.272(2) | 0.430(2) | 0.274(1) | 3.5(5)[a] |
| C23′ | −0.240(4) | 0.327(4) | 0.271(3) | 6(1)[a] |
| C24 | −0.232(2) | 0.225(2) | 0.335(2) | 4.2(6)[a] |
| C24′ | −0.207(3) | 0.182(3) | 0.394(2) | 4.0(8)[a] |
| C25 | 0.208(2) | −0.024(1) | 0.0116(9) | 4.9(4) |
| C26 | 0.369(2) | 0.024(2) | 0.063(1) | 3.5(5)[a] |
| C26′ | 0.328(3) | 0.090(3) | 0.066(2) | 3.7(8)[a] |
| C27 | 0.119(3) | 0.154(1) | 0.058(1) | 8.9(8) |
| C28 | −0.035(1) | 0.046(1) | 0.176(1) | 4.7(4) |
| C29 | 0.077(1) | −0.146(1) | 0.141(1) | 4.5(4) |
| C30 | 0.099(1) | −0.118(1) | 0.2764(9) | 6.7(4) |
| C31 | 0.390(2) | −0.244(2) | 0.380(1) | 4.0(5)[a] |
| C31′ | 0.365(4) | −0.152(3) | 0.426(3) | 2.9(9)[a] |
| C32 | 0.439(2) | −0.114(2) | 0.452(1) | 4.9(5)[a] |
| C32′ | 0.521(4) | −0.093(4) | 0.446(3) | 3.0(9)[a] |
| C33 | 0.608(2) | −0.287(1) | 0.408(1) | 4.7(4) |
| C34 | 0.592(2) | 0.021(2) | 0.205(1) | 4.0(5)[a] |
| C34′ | 0.608(4) | −0.045(4) | 0.171(3) | 3(1)[a] |
| C35 | 0.635(2) | −0.010(2) | 0.349(1) | 3.9(5)[a] |
| C35′ | 0.638(4) | −0.015(3) | 0.296(2) | 2.5(8)[a] |
| C36 | 0.738(1) | −0.174(1) | 0.273(1) | 4.0(4) |
| C37 | 0.608(2) | 0.636(2) | 0.069(2) | 6.6(7)[a] |
| C37′ | 0.509(5) | 0.567(5) | 0.117(4) | 4(1)[a] |
| C38 | 0.497(2) | 0.662(2) | 0.017(2) | 9.2(7)[a] |
| C39 | 0.480(2) | 0.717(2) | −0.051(1) | 6.2(5)[a] |
| C40 | 0.366(2) | 0.737(2) | −0.100(1) | 7.6(6)[a] |
| C41 | 0.280(2) | 0.695(2) | −0.069(1) | 7.6(6)[a] |
| C42 | 0.318(2) | 0.633(2) | 0.008(2) | 10.6(8)[a] |
| C43 | 0.414(2) | 0.609(1) | 0.052(1) | 5.7(4)[a] |

[a] These atoms were left with isotropic thermal parameters, as they are involved in the disorder.

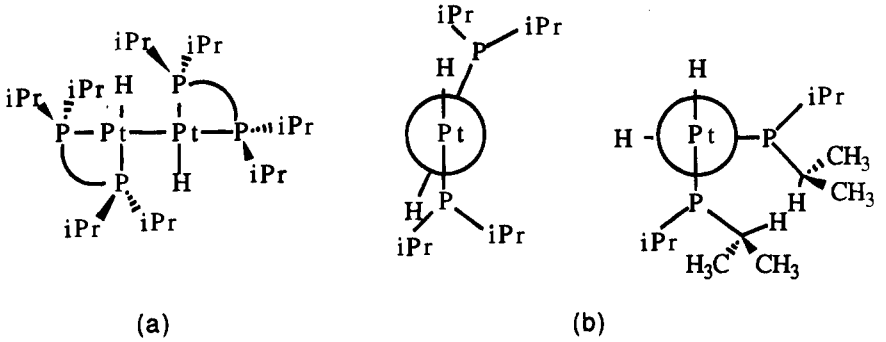


**Figure 3.** (a) Idealized geometry of **1** that would minimize steric interactions between the alkyl groups of the phosphine ligands and (b) Newman projections of both the 180 and 90° geometries, down the P−Pt−Pt−P vector, showing the increased steric interactions in the latter conformation (for clarity, the P nuclei *trans* to the Pt centers are not shown). Note the orientation of the isopropyl methine H's, as in the solid state structure of **1**, minimizing the steric interactions.

**Table 6.** Selected Intramolecular Distances (Å) and Angles (deg) in $[(dippe)PtH]_2$ (**1**) and $[(dtbpe)PtH]_2$ (**3**)

| | **1** | **3** |
|---|---|---|
| Pt(1)−Pt(2) | 2.5777(5) | 2.6094(6) |
| Pt(1)−P(1) | 2.257(3) | 2.274(3) |
| Pt(1)−P(2) | 2.242(3) | 2.248(3) |
| Pt(2)−P(3) | 2.254(3) | 2.281(3) |
| Pt(2)−P(4) | 2.244(3) | 2.260(3) |
| Pt(1)−Pt(2)−P(3) | 102.12(8) | 114.71(8) |
| Pt(1)−Pt(2)−P(4) | 167.43(8) | 153.75(9) |
| Pt(2)−Pt(1)−P(1) | 100.53(7) | 115.70(8) |
| Pt(2)−Pt(1)−P(2) | 168.59(9) | 152.31(9) |
| P(1)−Pt(1)−P(2) | 88.56(10) | 89.76(12) |
| P(3)−Pt(2)−P(4) | 88.23(11) | 89.58(11) |

The main difference between the Ni and Pd dimers and **1** is the presence of terminal hydrides in the latter complex, resulting in more acute P(1)−Pt(1)−Pt(2) and P(3)−Pt(2)−Pt(1) angles, making the 180° geometry the sterically favored one, relative to the 90° geometry (Figure 3). While the 180° geometry appears to be favored on steric grounds, the 90° geometry is assumed to be the thermodynamically preferred conformation, as it is observed in the solid state structures of **1** and **3**.

The structure of **3** is qualitatively similar to that of **1**; however, there are several differences. The Pt(1)−Pt(2) distance in **3** is 2.609(1) Å, 0.03 Å longer than in **1**. This lengthening is most reasonably ascribed to steric interactions between the larger *tert*-butyl groups on the two phosphine ligands, specifically between the C(6) and C(9) *tert*-butyl groups. In contrast to **1**, in which the methine hydrogens on these analogous carbon atoms can be oriented so as to minimize steric interactions, such a lower energy conformation does not exist for **3**. In addition, the P−Pt−Pt angles (114.7° for P(3)−Pt(2)−Pt(1), 115.7° for P(1)−Pt(1)−Pt(2), 152.3° for P(2)−Pt(1)−Pt(2), and 153.8° for P(4)−Pt(2)−Pt(1) deviate from the ideal square planar values by *ca.* 26°, *vs ca.* 13° in **1**. This distortion is also consistent with steric interactions between the *tert*-butyl groups.

The P(1)−Pt(1)−Pt(2)−P(3) torsional angle may also be used as evidence that steric interactions play a role in the structural distortions in **3**. In **3**, this angle is 108°, in **1**, it is 97°. The steric interactions between the C(6) and C(9) *tert*-butyl groups (on P(1) and P(3)) result in an opening of this angle by 11°, relative to **1**. There are no close intramolecular nonbonded interactions between the C(6) and C(9) alkyl groups, presumably because the distortions discussed above relieve such interactions. This is illustrated clearly by the observation that the C(17)−C(27) distance (methyl carbons on C(6) and C(9), respectively), 3.80 Å, decreases to 2.25 Å when the P−Pt−Pt angles, Pt−Pt distance, and P−Pt−Pt−P dihedral angles are set equal to their analogous values in the structure of **1**.

It can be argued that all of these distortions are also consistent with a distortion toward a bridging hydride structure for **3**. However, the solid state infrared data show that the hydrides are terminal in both **1** and **3**. No terminal M−H stretches are present in the infrared spectrum of $[(dcypp)Ni(\mu\text{-}H)]_2$;[7a] unfortunately, no infrared data were reported for $[(dippp)Pd(\mu\text{-}H)]_2$.[7c] Also, if the solid state structure of **3** did contain bridging or semibridging hydride ligands, the P(1)−Pt(1)−Pt(2)−P(3) torsional angle would be closer to 180°,[9] as is observed in Fryzuk's palladium analogue,[7c] to satisfy the square planar coordination of the platinum centers. The observed angle is 108.1°. It seems reasonable to conclude that the distortions observed in the structure of **3** arise as a result of the steric interactions discussed above.

**Room-Temperature NMR Spectra.** The room-temperature $^1H$, $^{31}P\{^1H\}$, and $^{195}Pt\{^1H\}$ (INEPT) NMR spectra of **1** (Figure 4) show that all four phosphorus nuclei, both platinum nuclei, and the two hydride nuclei are equivalent on the NMR time scale. Qualitatively, the room-temperature $^1H$ and $^{31}P\{^1H\}$ spectra of **2** and **3** are identical with those of **1**. The $^1H$, $^{31}P\{^1H\}$, $^{195}Pt\{^1H\}$ spectra for **1**−**3** consist of the superposition of three subspectra, arising from the three different isotopomeric combinations of platinum nuclei having different nuclear spins (Pt/Pt 43.8%, Pt/$^{195}$Pt 44.8%, $^{195}$Pt/$^{195}$Pt 11.4%; the percentages arise from the 33.8% natural abundance of $^{195}$Pt). The splitting of the $^1H$ spectrum consists of an apparent quintet of quintets (Figure 5), arising from the superposition of an $A_2M_2M'_2$ spin system (Pt/Pt isotopomer, central quintet), an $A_2M_2M'_2X$ spin system (Pt/$^{195}$Pt isotopomer, doublet of quintets), and an $A_2M_2M'_2XX'$ spin system ($^{195}$Pt/$^{195}$Pt isotopomer, triplet of quintets); the superposition of these spin systems, giving the observed apparent quintet of quintets, has been discussed in detail in the literature, with respect to $[(P\text{-}P)_2Pt_2H_3]^+[X]^-$ complexes.[3b,5e]

The pattern observed in the $^{31}P\{^1H\}$ spectrum (Figure 4b) arises from a combination of an $A_2A'_2$ spin system (Pt/Pt isotopomer, a singlet), an $A_2A'_2X$ spin system (Pt/$^{195}$Pt isotopomer, giving rise to all of the observed splitting in the

(9) (a) Boag, N. M.; Browning, J.; Crocker, C.; Goggin, P. L.; Goodfellow, R. J.; Murray, M.; Spencer, J. L. *J. Chem. Res. Synop.* **1978**, 228. (b) Boag, N. M.; Browning, J.; Crocker, C.; Goggin, P. L.; Goodfellow, R. J.; Murray, M.; Spencer, J. L. *J. Chem. Res. Miniprint* **1978**, 2962. (c) Yamamoto, Y.; Takahashi, K.; Yamazaki, H. *Chem. Lett.* **1985**, 201. (d) Couture, C.; Farrar, D. H.; Fisher, D. S.; Gukathasan, R. R. *Organometallics* **1987**, *6*, 532.

(10) Otsuka, S.; Yoshida, T.; Matsumoto, M.; Nakatsu, K. *J. Am. Chem. Soc.* **1976**, *98*, 5850.

(11) Bell, J. D.; Hall, D.; Waters, T. N. *Acta Crystallogr.* **1966**, *21*, 440.

(12) Anderson, G. K. *Adv. Organomet. Chem.* **1993**, *35*, 1.

(13) (a) Ciriano, M.; Green, M.; Howard, J. A. K.; Proud, J.; Spencer, J. L.; Stone, F. G. A.; Tsipis, C. A. *J. Chem. Soc., Dalton Trans.* **1978**, 801. (b) Green, M.; Howard, J. A. K.; Proud, J.; Spencer, J. L.; Stone, F. G. A.; Tsipis, C. A. *J. Chem. Soc., Chem. Commun.* **1976**, 671.

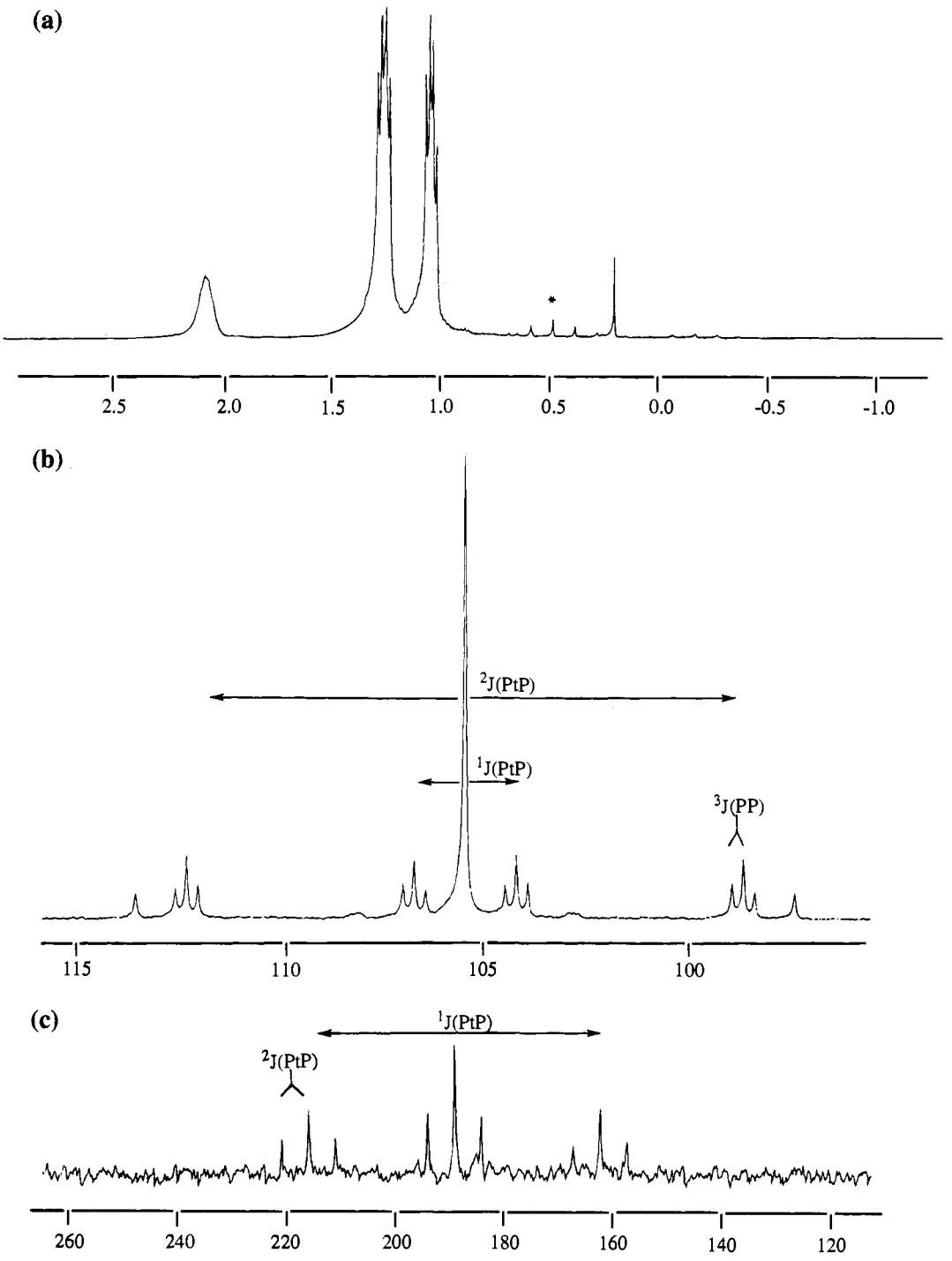


**Figure 4.** NMR spectra of **1** (25 °C, $C_6D_6$). Part a shows the $^1H$ spectrum (400 MHz). The central hydride resonance is indicated with an asterisk, and the outermost resonances are not resolved due to their low intensity. Part b shows the $^{31}P\{^1H\}$ spectrum (162 MHz). Part c shows the $^{195}Pt\{^1H\}$ INEPT spectrum (85.6 MHz).

experimental spectrum; see labels in Figure 4b), and an $A_2A'_2$-XX′ spin system ($^{195}Pt/^{195}Pt$ isotopomer, a second order pattern), the latter of which is only partially observed in the experimental spectrum (the outermost visible lines correspond to half of the total intensity of this subspectrum),[3b] as a result of the 11.4% abundance of this isotopomer and of the multiple couplings present for this spin system. Again, the superposition of these spin systems has been discussed in the literature, with respect to $[(P\text{-}P)_2Pt_2H_3]^+[X]^-$ complexes.[3b,5e] Similarly, the experimental $^{195}Pt\{^1H\}$ spectrum (Figure 4c) is a superposition of $A_2A'_2X$ ($Pt/^{195}Pt$, triplet of triplets, see labels on Figure 4c) and $A_2A'_2XX'$ ($^{195}Pt/^{195}Pt$, second order pattern) spin systems; the latter subspectrum is not observed in the experimental spectrum, due to its low relative abundance and multiple couplings. As expected, the $^{1,2}J_{PtP}$ values obtained from the $^{31}P\{^1H\}$ spectrum (Table 1) are identical to those measured from the $^{195}Pt\{^1H\}$ spectrum.

Clearly, some sort of fluxional process is occurring that makes the two hydrides, the four phosphorus nuclei, and the two platinum nuclei equivalent on the NMR time scale at room temperature, as the spectra are not consistent with the solid state structures of **1** and **3**. Such a process, in which there is equivalency within the sets of H, P, and Pt nuclei, has been reported for several $[(P\text{-}P)_2Pt_2H_3][X]$ complexes,[3b,5e] A static planar $[(P\text{-}P)Pt(\mu\text{-}H)]_2$ structure of $D_{2h}$ symmetry is not consistent with the observed equivalency, although this has been suggested in the literature.[4a,7c]

The NMR values for **1**–**3** (Table 1) are similar to the room-

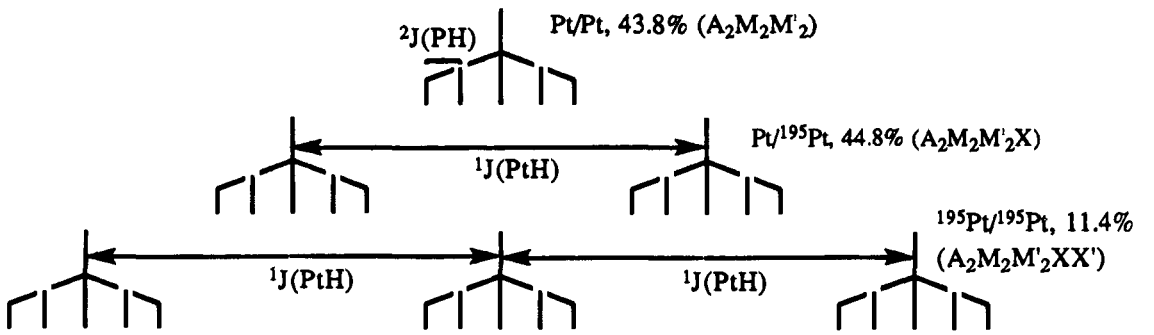


**Figure 5.** Splitting diagram for the hydride region of the 25 °C $^1$H spectrum of **1** (Figure 4a, an apparent "quintent of quintets").

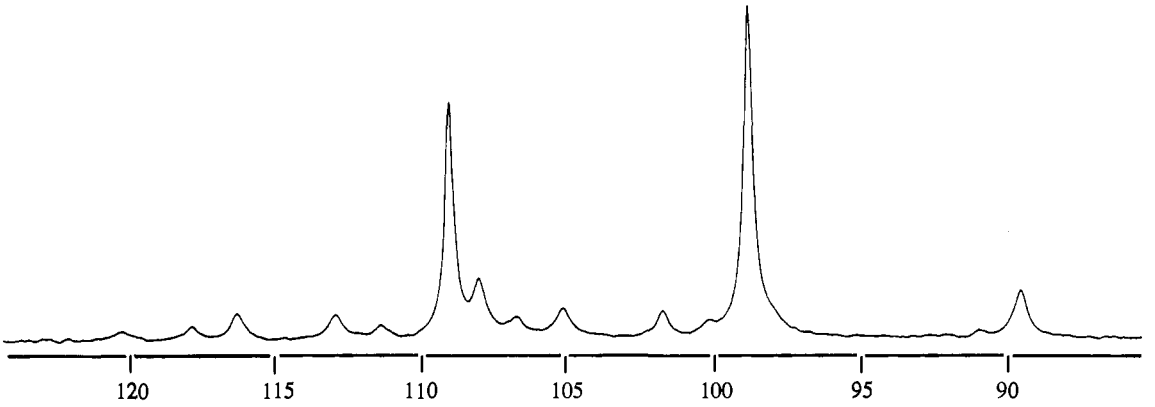


**Figure 6.** $^{31}$P{$^1$H} NMR spectrum of **1** at −90 °C (121 MHz, toluene-$d_8$).

**Table 7.** $^1$H and $^{31}$P{$^1$H} NMR Data for Selected [(P-P)$_2$Pt$_2$H$_3$][X] Complexes in $CDCl_3$

| complex | $\delta$ (Pt−H), ppm | $^2J_{PH}$, Hz | $^1J_{PtH}$, Hz | $\delta$ (P), ppm | $^1J_{PtP}$, Hz | $J_{PP}$, Hz | reference |
|---|---|---|---|---|---|---|---|
| [(dcype)$_2$Pt$_2$H$_3$][OH] | −2.81 | 39 | 480 | 84.2 | 2802, 149 | 8 | this work |
| [(dppe)$_2$Pt$_2$H$_3$][BF$_4$] | −2.8 | 41 | 500 | 57.2 | 2925, 171 | 10 | 5e |
| [(dtbpe)$_2$Pt$_2$H$_3$][BPh$_4$] | −3.85 | 40 | 443 | 109 | 2946, 161 | 8 | 3b |

temperature values reported by Pidcock and co-workers for [(dppe)PtH]$_2$ (also in Table 1).[4b] Comparison of these values to the values for trihydride cationic complexes of the type [(P-P)$_2$Pt$_2$H$_3$][X] (Table 7) which exhibit several different structures,[5e] all of which contain at least one bridging hydride in the solid state, shows significant differences. The neutral dimers **1**−**3** have a much larger average $^3J_{PP}$ value than the average long-range $J_{PP}$ value for the cationic complexes. In addition, the average $^2J_{PtP}$ value for the neutral dimers **1**−**3** is much larger than the analogous value for the cationic complexes (*e.g.*, $^2J_{PtP}$ = 420 Hz for **2**; $J_{PtP}$ = 149 Hz for the analogous cationic complex, [(dcype)$_2$Pt$_2$H$_3$][OH]). These differences indicate that there is more spin−spin communication between the two halves of the neutral dimers, relative to the cationic complexes. The direct, unbridged Pt−Pt bond in the solid state for the complexes **1**−**3** transmits spin−spin coupling more efficiently than the bridged Pt−Pt bond in the cationic complexes.

Comparison of the averaged spectral values for the neutral dimers to those of monomeric *cis*-P$_2$PtH$_2$ (Table 2) shows that the $^1J_{PtH}$ values are much smaller, and that the $^1J_{PtP}$ values are larger, for the former complexes. These differences are indicative of bridging or semibridging hydride ligands in the neutral dimers (on the NMR time scale, at room temperature),[14] inconsistent with the terminal hydride coordination found in the solid state structures of **1** and **3**. Lastly, comparison of the values among the three dimers shows that **1** and **2** possess very similar values, while the values for **3** are slightly different (this difference being most pronounced in the $J_{PtP}$ values).

**Low-Temperature NMR Spectra.** In order to learn more about the fluxional process, NMR samples of **1**, **2**, and **3** in toluene-$d_8$ were cooled to −90 °C, and the $^1$H and $^{31}$P{$^1$H} NMR spectra were recorded. The spectra of **3** were virtually identical with the room-temperature spectra, implying that the fluxional process is still rapid. However, the spectra of **1** and **2** were significantly different from the room-temperature spectra, due to the stopping of the fluxional process(es) that occur(s) at room temperature. The temperature at which the fluxional process is stopped is −54 °C for **1** and −36 °C for **2**. Both averaged[3b,5e] and stopped-exchange[5a,c,h,15] cases have been reported for [P$_4$-Pt$_2$H$_3$][X] complexes; complexes with chelating phosphines yield averaged spectra at all temperatures, and complexes with monodentate phosphines yield stereochemically rigid spectra at all temperatures. The palladium dimer [(dippp)PtH]$_2$ is fluxional at all temperatures.[7c] Thus, complexes **1** and **2** represent the first cases in which both regimes, fluxional and stereochemically rigid, are accessible. An interesting study[16] has yielded an estimate of 17.2 kJ mol$^{-1}$ for the fluxional process in [(dppe)$_2$-Pt$_2$H$_3$][BF$_4$], based on proton $T_1$ and $T_2$ measurements.

The $^{31}$P{$^1$H} spectrum of **1** taken at −90 °C is shown in Figure 6. The low-temperature $^1$H and $^{31}$P{$^1$H} spectra for **2** are qualitatively identical to those of **1**. While the 90 and 180° geometries (Figure 3) cannot be distinguished on the basis of the low-temperature $^1$H, $^{31}$P, and $^{195}$Pt NMR data, the data are entirely consistent with the solid state structure found for **1**, as discussed below, and so it is reasonable to assume that the low-

(14) Pregosin, P. S. In *Annual Reports on NMR Spectroscopy*; Webb, G. A., Ed.; Academic Press Inc.: London, 1986; Vol. 17.
(15) Bracher, G.; Grove, D. M.; Venanzi, L. M.; Bachechi, F.; Mura, P.; Zambonelli, L. *Angew. Chem., Int. Ed. Engl.* **1978**, *17*, 778.
(16) Aime, S.; Gobetto, R.; Bandini, A. L.; Banditelli, G.; Minghetti, G. *Inorg. Chem.* **1991**, *30*, 316.

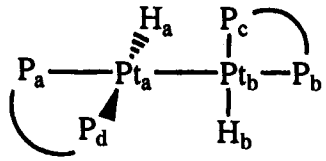


**Figure 7.** Assignments used to discuss the low-temperature NMR values of **1** and **2**.

temperature solution structure is similar to the observed solid state structure. Since the low-temperature spectra of **1** and **2** are similar, we assume that they have similar solid state structures.

The assignments shown in Figure 7 will be used to discuss the low-temperature spectra; unless otherwise stated, only one-half of the dimer will be explicitly discussed, the other half being related by a $C_2$ axis (*e.g.*, $^1J_{Pt_aH_a}$ implies $^1J_{Pt_bH_b}$; while the $^{195}$Pt/Pt isotopomer of the dimer does not possess a true $C_2$ axis, any exceptions will be explicitly stated when necessary). The low-temperature $^1$H and $^{31}$P{$^1$H} values for **1** and **2** are presented in Table 8.

The hydride region of the low-temperature $^1$H spectrum contains a doublet with symmetrically spaced satellites. This pattern arises from coupling to the *trans* phosphorus nucleus and to the nearer $^{195}$Pt nucleus ($^2J_{PtH_a}$ and $^1J_{Pt_aH_a}$, respectively). Comparison of these $J_{PtH}$ and $J_{PH}$ values to the analogous values for the *cis*-$P_2PtH_2$ complexes (Table 2) shows that, in contrast to the room-temperature values for the dimers (Table 1, and accompanying discussion), the values are very similar, providing support for a low-temperature structure containing terminal hydride ligands located *trans* to a phosphorus nucleus. The couplings between $H_a$ and the three other phosphorus nuclei and the other platinum center are presumably too small to be resolved.

The low-temperature $^{31}$P{$^1$H} spectrum (Figure 6) is also consistent with the solid state structure found for **1**. There are now two different phosphorus environments, $P_a/P_b$, which are *trans* to Pt centers, and $P_c/P_d$, which are *trans* to hydrides. Again, this spectrum is a superposition of the three subspectra arising from the three different isotopomers present. The Pt/Pt isotopomer gives two singlets, for the two different pairs of phosphorus environments (an AA′MM′ spin system), which are observed as the two major resonances in the experimental spectrum. The $^{195}$Pt/$^{195}$Pt subspectrum (an AA′MM′XX′ system) is not visible in the experimental spectrum due to its low relative abundance, and so the remainder of the spectrum arises from the Pt/$^{195}$Pt isotopomer (an AA′MM′X spin system). A splitting diagram for this spin system is shown in Figure 8.

The higher-field resonance is assigned to $P_c/P_d$; this assignment was confirmed by a $^1$H/$^{31}$P{$^1$H} HMQC[17] spectrum (included as supplementary material). The splitting observed is $^1J_{Pt_aP_d}$; $^2J_{Pt_bP_d}$ is unresolved. It is not very surprising that the P−P couplings are unresolved as the *cis* coupling $^2J_{P_aP_d}$ is expected to be the largest coupling involving $P_d$, and $^2J_{PP}$ values in *cis*-$P_2PtX_2$ complexes (X = H, R), where $P_2$ is a $C_2$-bridged chelating phosphine, can be <3 Hz.[18] The lower-field resonance arises from $P_a$ and $P_b$, which are *trans* to platinum centers. The two different $J_{PtP}$ values observed are $^1J_{Pt_aP_a}$ and $^2J_{Pt_bP_a}$; the additional coupling observed is $^3J_{P_aP_b}$ (Figure 8). This P−P coupling cannot be $^2J_{P_aP_d}$ since it is not seen in the higher-field resonance. Again, as for the high-field resonance, $^2J_{P_aP_d}$ and $^3J_{P_aP_c}$ are unresolved (this is partially a result of the relatively broad resonances in this spectrum, $w_{1/2} \approx 40$ Hz). Simulation of the experimental spectrum using these assignments gives good agreement with the experimental spectrum (the simulated spectrum and subspectra are available as supplementary material).

The $^{195}$Pt/$^{195}$Pt subspectrum (an AA′MM′XX′ spin system) is not visible in the $^{195}$Pt dimension of the experimental $^1$H/$^{195}$Pt{$^1$H} HMQC[17] spectrum, and consequently, the entire experimental spectrum arises from the Pt/$^{195}$Pt subspectrum (an AA′MM′X spin system). Simulation of this subspectrum, using the coupling constant values obtained from the $^{31}$P{$^1$H} spectrum, gives good agreement with the experimental spectrum (the experimental spectrum, simulated subspectra, and simulated spectrum are available as supplementary material), providing further support that the low-temperature solution state structure of **1** is identical to the solid state structure.

**Solution Behavior of 1−3.** A 1:1 mixture of **5** and its deuterated analogue, (dcype)$PtD_2$ (**5**-$d_2$), in $C_6D_6$ reaches the 1:2:1 **5**:(dcype)Pt(H)(D):**5**-$d_2$ equilibrium ratio within 1 h. The same result was found for the analogous reaction using **6** and its deuterated derivative. In both cases, the reactions were followed by $^{31}$P{$^1$H} and $^1$H NMR spectroscopy. As a control, no evidence of H/D scrambling in the protiated monomers **5** and **6** with $C_6D_6$ at room temperature was observed in the $^1$H and $^{31}$P{$^1$H} spectra over several days. In contrast, a 1:1 sample of **1** and its deuterated analogue, [(dippe)PtD]$_2$ (**1**-$d_2$), scrambles much more slowly than the monomers; the half-life is *ca.* 90 h at room temperature (eq 2). Dimer **1** does not undergo H/D

$$\underset{\textbf{1}\text{-}d_2}{[(\text{dippe})\text{PtD}]_2} + \underset{\textbf{1}}{[(\text{dippe})\text{PtH}]_2} \xrightarrow[C_6D_6,\ rt]{} \begin{matrix}\text{slow H/D}\\ \text{scrambling}\\ (t_{1/2}\ ca.\ 90\ h)\end{matrix} \quad (2)$$

exchange with $C_6D_6$ at room temperature at any appreciable rate. However, heating a $C_6D_6$ solution of **1**, **2**, or **3** for 12 h at 90−100 °C results in complete deuterium incorporation at the hydride positions, for all three samples.

We have not quantitatively studied the scrambling process; however, several qualitative experiments were done. No evidence of scrambling was observed for a 1:1 sample of **3** and **6**-$d_2$ after 51 h at room temperature (eq 3). A 1:1 sample of **1**

$$\underset{\textbf{6}\text{-}d_2}{(\text{dtbpe})\text{PtD}_2} + \underset{\textbf{3}}{[(\text{dtbpe})\text{PtH}]_2} \xrightarrow[C_6D_6,\ rt/51\ h]{} \begin{matrix}\text{no H/D}\\ \text{scrambling}\end{matrix} \quad (3)$$

$$\underset{\textbf{6}\text{-}d_2}{(\text{dtbpe})\text{PtD}_2} + \underset{\textbf{1}}{[(\text{dippe})\text{PtH}]_2} \xrightarrow[C_6D_6,\ rt/48\ h]{} \begin{matrix}\text{complete H/D}\\ \text{scrambling}\end{matrix} \quad (4)$$

$$\underset{\textbf{1}\text{-}d_2}{[(\text{dippe})\text{PtD}]_2} + \underset{\textbf{3}}{[(\text{dtbpe})\text{PtH}]_2} \xrightarrow[C_6D_6,\ rt/72\ h]{} \begin{matrix}\text{no H/D}\\ \text{scrambling}\end{matrix} \quad (5)$$

and **6**-$d_2$ in $C_6D_6$ scrambles completely within 48 h (eq 4). Also, no evidence of scrambling is observed for a 1:1 sample of **1**-$d_2$ and **3** after 72 h (eq 5). Clearly, there are differences in the reactivity of **1**, relative to that of **3**. The lower rates in **3** are likely due to the increased steric protection of the Pt−Pt bond by the *tert*-butyl groups, as discussed in detail in the structural discussion above.

A small amount of "mixed dimer", [$(R_2P(CH_2)_2PR_2)$(H)Pt−Pt(H)$(R'_2P(CH_2)_2PR'_2)$], was present in the samples for which H/D scrambling was observed. The identity of these mixed dimers was confirmed by a $^1$H/$^{31}$P{$^1$H} HMQC[17] NMR spectrum on a sample containing a mixture of **1**, **2**, and [(dippe)-

(17) (a) Bax, A.; Griffey, R. H.; Hawkins, B. L. *J. Magn. Reson.* **1983**, *55*, 301. (b) Bax, A.; Subramanian, S. *J. Magn. Reson.* **1986**, *67*, 565.

(18) Garrou, P. E. *Chem. Rev.* **1985**, *85*, 171. (b) Hackett, M.; Ibers, J. A.; Whitesides, G. M. *J. Am. Chem. Soc.* **1988**, *110*, 1436.

Table 8. $^1H$ and $^{31}P\{^1H\}$ NMR Data for **1** and **2** (−90 °C, toluene-$d_8$)

| | δ (Pt−H), ppm | $^2J_{PdHa}$, Hz | $^1J_{PtaHa}$, Hz, | δ (P), ppm | $^1J_{PtaPa}$, Hz | $^2J_{PtaPb}$, Hz | $^2J_{PtaPc}$, Hz | $^1J_{PtaPd}$, Hz | $^3J_{PaPb}$, Hz |
|---|---|---|---|---|---|---|---|---|---|
| **1** | 1.04 | 163 | 996 | 109.1, 98.5 | 2030[a] | 785 | *b* | 2320 | 200[c] |
| **2** | *d* | 170 | *d* | 96.9, 90.1 | 2000 | 800 | *b* | 2320 | 210 |

[a] All of the $J_{PtP}$ values in this table were measured from the Pt/$^{195}$Pt subspectrum, as the Pt/Pt subspectrum has no $^{195}$Pt and the $^{195}$Pt/$^{195}$Pt subspectrum is not visible in the experimental spectrum. [b] Unresolved, see text. [c] The $^3J_{PaPb}$ values arise from the Pt/$^{195}$Pt and $^{195}$Pt/$^{195}$Pt subspectra and were measured from the former subspectrum. [d] Due to the cyclohexyl resonances obscuring the hydride resonance, these values could not be measured. Only the higher field platinum satellite (a doublet) was visible.

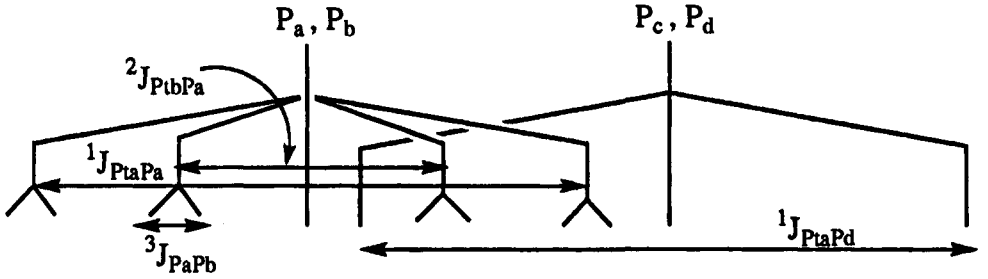


**Figure 8.** Proposed coupling scheme for the low-temperature $^{31}P\{^1H\}$ $^{195}$Pt/Pt subspectrum (AA'MM'X spin system) of **1**.

(H)Pt−Pt(H)(dcype)] (made by heating a $C_6H_6$ sample of **1** and **2**); three different hydride resonances were correlated with the three different dimeric complexes present (this spectrum is available as supplementary material). While no more than *ca.* 10−20% of this mixed dimer was present in the samples, it may be responsible for the H/D scrambling that occurs. The mechanism of formation of such mixed dimers was not investigated; however, on the basis of the low liability of bidentate phosphine ligands bound to platinum, it is not unreasonable to postulate that it involves cleavage of the Pt−Pt bond to generate $P_2Pt$ and $P_2PtH_2$ fragments, which can then scramble to give the mixed dimer.

## Discussion

**Fluxional Behavior.** Any postulate concerning the fluxionality of these dimers must adequately explain the equivalence of all four phosphorus nuclei, both hydrides, and both platinum centers in the rapid exchange temperature region. In addition, the proposed process must be consistent with the lower barrier observed for the derivative with the bulkiest phosphine, **3**. The simplest process that is consistent with these observations (Figure 9) involves rotation of one of the ($P_2PtH$) moieties by 90° around the Pt−Pt vector (step A) to give the 180° geometry discussed above (Figure 3), followed by hydride exchange between metal centers with simultaneous twisting of the phosphine ligands by 90° relative to the plane defined by the square planar metal centers (step B). Such a fluxional process, if fast on the NMR time scale, would result in equivalent hydrides and would exchange $P_a$ and $P_b$ with $P_d$ and $P_c$, respectively, making all four phosphorus nuclei equivalent.

If it is assumed that the first stage of the process depicted above (step A) has the higher barrier, with the hydride exchange/phosphine-twisting process (Step b) possessing a relatively small barrier, then stopping the fluxional process is a result of freezing out the conformation that is observed in the solid state, *i.e.*, a geometry in which the two square planes of the platinum coordination spheres are oriented roughly 90° relative to each other. As discussed above, the low-temperature NMR data are consistent with the solid state geometry. If the 180° orientation were frozen out, then hydride exchange between the platinum centers would not cease, as the barrier to this process (*B*) is assumed to be small. Consistent with the assumption that the 90° orientation is thermodynamically more stable than the 180° orientation is the fact that both **1** and **3** crystallize in the former geometry.

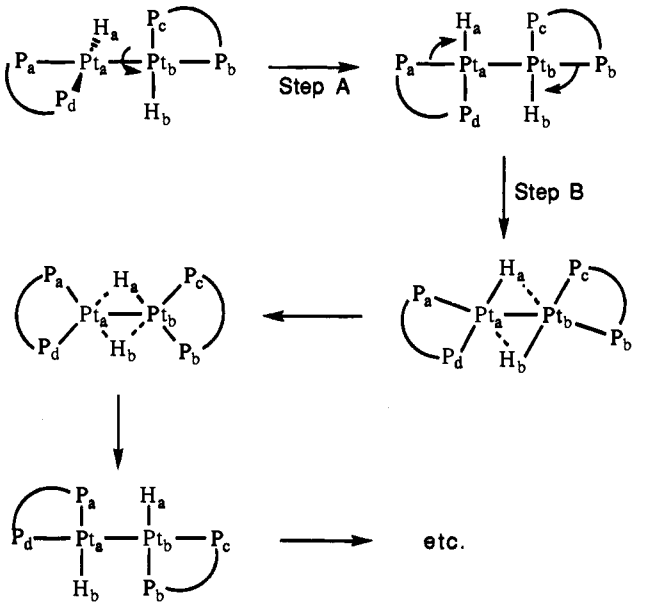


**Figure 9.** Proposed fluxional process for the dimers **1**, **2**, and **3**.

Why, though, does **3** have a lower barrier for the fluxional process (*i.e.*, step A) than **1** and **2**? As discussed above, there are several distortions in the solid state structure of **3**, relative to that of **1**, that were rationalized as being due to increased steric interactions between the *tert*-butyl groups. These distortions indicate that the 90° orientation for **3** is destabilized, relative to the analogous orientation for **1**. This destabilization would result in a lower barrier to interconversion between the 90 and 180° orientations for **3** (Figure 10), as is experimentally observed. This argument assumes that the thermodynamic stability of the 180° orientation for all three dimers is roughly equal; *i.e.*, the destabilization of the 90° orientation of **3** is not offset by a corresponding destabilization of the 180° geometry. This seems reasonable to us, as this geometry minimizes steric interactions between the alkyl groups.

The similar barriers for **1** and **2** are consistent with this proposal as the phosphine on **2** (dcype), as in the case of **1**, also possesses a methine hydrogen which can be oriented in such a way as to relieve steric interactions between alkyl groups (Figure 3). As discussed above, this stabilizes the 90° geometry. The close agreement of the room-temperature NMR values for **1** and **2**, relative to the slightly different values for **3** (Table 1), may also be indicative of these differences.

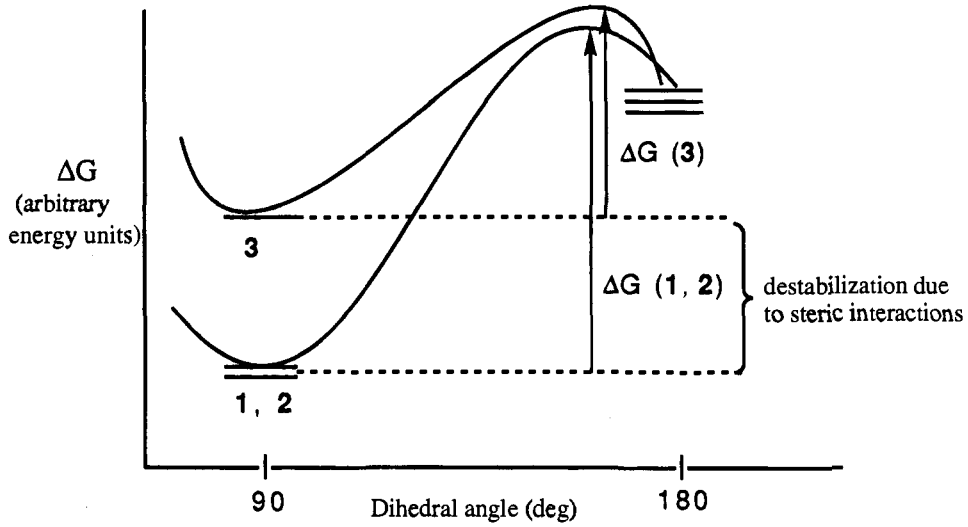


**Figure 10.** Illustration of the proposed cause of the differences in the fluxional barriers for **1**, **2**, and **3**.

**(P-P)$PtH_2$/$[(P\text{-}P)PtH]_2$ Equilibria.** Theoretical calculations have shown that there is essentially no barrier to reductive elimination of dihydrogen from *cis*-$P_2PtH_2$ complexes.[19] Otsuka and co-workers have suggested that bulky phosphines kinetically stabilize the *cis*-dihydride monomers, thus allowing their isolation.[3a,b] The results described above support this explanation; the stability of the monomeric *cis*-dihydride complexes that we have prepared (*i.e.*, the tendency not to dimerize in solution) correlates directly with the steric size of the phosphine (**3** > **2** > **1**; the cone angles for the monodentate analogues, $PR_3$, are 182, 170, and 160°, for $P(tBu)_3$, $PCy_3$, and $P(iPr)_3$, respectively[20]).

For *cis*-dihydrides containing sterically smaller phosphine ligands (*e.g.*, **4**), the kinetic barrier for loss of $H_2$ is small and occurs in solution at room temperature. The resulting product of such a reaction is a neutral $[(P\text{-}P)PtH]_2$ dimer, presumably arising from reaction of *cis*-$P_2PtH_2$ with $P_2Pt$, although other mechanisms of formation of the dimeric complexes are possible. This contrasts with the postulate made by Otsuka *et al.*[3a] that loss of dihydrogen from *cis*-$P_2PtH_2$ complexes gives solutions of $(P_2Pt)_2$ dimers. The Otsuka postulate was based on several lines of evidence: the structure of $[(dtbpp)Pt]_2$, which showed no evidence for hydrides; a decrease in the intensity of the hydride resonance in the $^1H$ NMR spectra and the M−H stretch in the IR spectrum as solutions of the *cis*-dihydride monomers were heated; and a color change from colorless to reddish-brown as the solutions were heated. The last three observations are also consistent with loss of dihydrogen to give $(P_2PtH)_2$ dimers, as we have shown.

In contrast to the reddish-brown solutions formed upon heating solutions of *cis*-$P_2PtH_2$ complexes, the $(P_2Pt)_2$ dimer was prepared by the sodium amalgam reduction of a THF solution of $(dtbpp)PtCl_2$ under nitrogen. As mentioned by Otsuka *et al.*, it is possible that a *cis*-$P_2PtH_2$ intermediate is never formed in this reaction and that the $(P_2Pt)_2$ dimer results from reduction of the $P_2PtCl_2$ starting material to a $P_2Pt$ intermediate, which then dimerizes to give the observed product. On the basis of the results presented above, the formation of $(P_2Pt)_2$ dimeric complexes from solutions of *cis*-$P_2PtH_2$ complexes is not a general process; formation of Pt(I) hydride-containing dimers such as **1**−**3** is favored, at least with the chelating phosphines used in this study.

The geometry of these $[(P\text{-}P)MH]_2$ dimers changes on descending the group 8 metals; the hydrides in the Ni complex are symmetrically bridging,[7b] those in the Pd complex are semibridging,[7c] and those in the Pt complexes described above are strictly terminal. This may be rationalized as a relativistic effect in the following way.[21] In the gas phase, the Au−H distance of 1.52 Å is less than the Ag−H distance of 1.62 Å, even though the M−M distances in the homonuclear diatomic molecules are virtually identical ($d$(Ag−Ag) = 2.48 Å, $d$(Au−Au) = 2.47 Å). This has been rationalized on the basis of the relativistic stabilization of the 6s orbital of Au *vs* the 5s orbital of Ag.[21c] Since terminal M−H bonds are shorter than bridging M−H bonds, they can incorporate more metal-based s orbital character. This seems to be a reasonable rationalization for why M−H terminal bonds are preferred as one descends the Ni/Pd/Pt column.

## Experimental Section

**Apparatus and Materials.** All reactions and product manipulations were carried out under dry nitrogen using standard Schlenk and drybox techniques. Pentane, hexane, toluene, diethyl ether, and tetrahydrofuran were distilled from sodium benzophenone ketyl under nitrogen immediately prior to use. Dichloromethane was distilled from calcium hydride under nitrogen immediately prior to use. Deuterated solvents for NMR measurements were distilled from either sodium or potassium under nitrogen and stored over sodium. Other chemicals were of reagent grade, unless otherwise specified.

Infrared spectra were recorded on a Nicolet 5DX FTIR spectrometer as Nujol mulls between CsI plates. Melting points were measured on a Thomas-Hoover melting point apparatus in capillaries sealed under nitrogen and are uncorrected. Elemental analyses were performed by the microanalytical laboratories at the University of California, Berkeley. Mass spectrometry analyses were obtained at the UCB mass spectrometry facility on a Kratos MS-50 mass spectrometer, and the isotopic cluster of the molecular ion is reported as ion amu (observed intensity, calculated intensity).

All $^1H$, $^{31}P\{^1H\}$, $^{195}Pt\{^1H\}$, and 2-D NMR spectra were recorded on Bruker AM and AMX spectrometers operating at 400, 162, or 85.6 MHz, respectively, or at 300, 121.5, or 64.2 MHz, respectively. The 2-D spectra were acquired using the heteronuclear multiple quantum coherence (HMQC) pulse sequence.[17] $^1H$ NMR shifts are relative to tetramethylsilane, and the residual protio-resonance was used as an internal reference; $^{31}P$ NMR shifts are relative to 85% $H_3PO_4$ at $\delta$ 0.0, with shifts downfield of the reference considered positive. $^{195}Pt$ shifts

(19) (a) Low, J. J.; Goddard, W. A., III. *J. Am. Chem. Soc.* **1984**, *106*, 6928. (b) Low, J. J.; Goddard, W. A., III. *Organometallics* **1986**, *5*, 609.
(20) Otsuka, S. *J. Organomet. Chem.* **1980**, *200*, 191.
(21) (a) Pitzer, K. *Acc. Chem. Res.* **1979**, *12*, 271. (b) Pyykko, P.; Desclaux, J. P. *Ibid.* **1979**, *12*, 276. (c) Pyykko, P. *Chem. Rev.* **1988**, *88*, 563.

are referenced to a frequency scale in which the proton signal of tetramethylsilane is at 100.000 MHz and the frequency of 0.0 ppm for $^{195}Pt$ is set to 21.4000 MHz[14] and scaled according to the $^1H$ frequency of the particular machine used.

The (P-P)$PtCl_2$ complexes were made from (cod)$PtCl_2$ and the corresponding phosphines. Otsuka's method was used to prepare *cis*-(dtbpe)$PtH_2$ (**6**).[3a] *cis*-(dcype)$PtH_2$ (**5**) was prepared *via* the same procedure, using (dcype) as the phosphine; its spectroscopic properties were identical to those reported in the literature.[4a] The deuterated analogue, (dcype)$PtD_2$, (**5**-$d_2$), was prepared in the same manner, using deuterium gas instead of hydrogen gas.

**[(dippe)PtH]$_2$ (1).** A mixture of (dippe)$PtCl_2$ (1.2 g, 2.3 mmol) and Na/Hg (0.8%, 50 g) in THF (150 mL) was stirred under $H_2$ (1 atm) at room temperature for 15 h. The mixture was allowed to settle for 4 h and filtered, and the solvent was removed from the filtrate under reduced pressure. The dark brown solid was extracted with hexane (3 × 50 mL), the solution was filtered, and the filtrate was concentrated to *ca.* 40 mL. Slow cooling of this solution to −40 °C yielded **1** as light brown crystals (0.65 g, 62%), mp 118−131 °C dec. $^1H$ NMR ($C_6D_6$): δ 2.06 (m, 8H), 1.40−1.00 (m, 56H), 0.50 ("q of q", 2H, $^1J_{PtH}$ = 516 Hz, $^2J_{PH}$ = 40 Hz) ppm. $^{31}P\{^1H\}$ NMR, see Table 1. $^{195}Pt\{^1H\}$ NMR (toluene-$d_8$): δ +190 ($^1J_{PtP}$ = 2210 Hz, $^2J_{PtP}$ = 410 Hz) ppm. IR: 1939 (s), 1926 (s), 1406 (m), 1378 (s), 1358 (s), 1298 (2), 1241 (s), 1234 (s), 1159 (w), 1104 (m), 1086 (m), 1076 (m), 1027 (s), 1021 (s), 923 (m), 887 (s), 882 (s), 856 (m), 853 (m), 776 (s), 680 (s), 672 (s), 660 (s), 652 (s), 634 (s), 577 (m), 514 (s), 481 (m), 465 (m), 440 (m) $cm^{-1}$. MS *m/z* (EI, 50 eV): 914.3 (43, 32), 915.3 (77, 72), 916.3 (100, 100), 917.3 (69, 76), 918.3 (48, 51), 919.3 (24, 26), 920.4 (17, 16), 921.3 (5, 4), 922.3 (2, 2). Anal. Calcd for $C_{28}H_{66}P_4Pt_2$: C, 36.7; H, 7.26. Found: C, 36.9; H, 7.23.

**[(dcype)PtH]$_2$ (2).** A toluene solution (50 mL) of **5** (0.90 g, 1.5 mmol) was heated at 110 °C for 16 h in a Schlenk tube which was kept under a slow flow of $N_2$. The flask was allowed to cool to room temperature, and the solvent was removed under reduced pressure, yielding a yellow solid. The $^{31}P\{^1H\}$ spectrum of the crude product showed the material was a 3:1 mixture of **2**:**5**. This residue was extracted with pentane (3 × 30 mL), the solvent was removed from the extract under reduced pressure, and the resulting solid was dissolved in THF (15 mL). Slow cooling of this solution to −80 °C yielded **2** as yellow crystals (0.53 g, 58%), mp 224−231 °C dec. $^1H$ NMR ($C_6D_6$): δ 2.38−0.82 (m, 96H), 0.49 (q of q, 2H, $^1J_{PtH}$ = 512 Hz, $^2J_{PH}$ = 40 Hz) ppm. $^{31}P\{^1H\}$ NMR, see Table 1. IR: 1965 (s), 1937 (s), 1445 (s), 1409 (w), 1378 (s), 1343 (m), 1301 (w), 1290 (w), 1262 (m), 1237 (w), 1187 (w), 1178 (m), 1169 (m), 1048 (m), 1004 (s), 913 (m), 887 (m), 853 (m), 851 (s), 818 (m), 780 (m), 739 (s), 648 (m), 638 (m), 537 (m), 523 (m), 501 (m), 458 (m) $cm^{-1}$. Anal. Calcd for $C_{52}H_{98}P_4Pt_2$: C, 50.5; H, 7.98. Found: C, 50.6; H, 8.04.

**[(dtbpe)PtH]$_2$ (3).** A 4:1 hexane:toluene solution (60 mL, total) of **6** (0.52 g, 1.0 mmol) was heated at 90 °C for 16 h in a Schlenk tube under a slow purge of $N_2$. The solvent was removed under reduced pressure from the reddish-brown solution, and the residue was extracted with hexane (3 × 30 mL). The solvent was removed from the extract under reduced pressure, and the solid residue was redissolved in toluene (20 mL). Slow cooling of this solution to −40 °C yielded **3** as dark orange prisms (0.38 g, 73%), mp 220−236 °C dec. $^1H$ NMR ($C_6D_6$): δ 1.50 (m, 8H), 1.35 (m, 72H), 0.05 (q of q, 2H, $^1J_{PtH}$ = 570 Hz, $^2J_{PH}$ = 42 Hz) ppm. $^{31}P\{^1H\}$ NMR, see Table 1. IR: 1975 (bm), 1951 (bm), 1479 (s), 1385 (s), 1363 (s), 1356 (s), 1261 (w), 1239 (w), 1182 (s), 1094 (m), 1019 (m), 937 (m), 851 (m), 812 (s), 775 (s), 664 (s), 651 (s), 644 (s), 602 (s), 570 (m), 495 (s), 458 (m), 423 (m) $cm^{-1}$. Anal. Calcd for $C_{36}H_{82}P_4Pt_2$: C, 42.0; H, 8.03. Found: C, 41.7; H, 7.96.

**[(dippe)PtD]$_2$ (1-$d_2$).** A mixture of (dippe)$PtCl_2$ (1.1 g, 2.1 mmol) and Na/Hg (0.8%, 50 g) in THF (150 mL) was stirred under $D_2$ (1 atm) at room temperature for 15 h. The mixture was allowed to settle for 4 h and filtered, and the solvent was removed from the filtrate under reduced pressure to yield a dark brown solid. A $^1H$ NMR spectrum at this point showed that the crude product was an isotopic mixture of the dideuteride, hydridodeuteride, and dihydride complexes. The solid was dissolved in toluene (80 mL) and stirred at room temperature under $D_2$ (1 atm) for 30 h. The head space over the solution was evacuated and refilled with 1 atm of $N_2$ gas, and the sample was stirred at room temperature for 70 h. This process was repeated ($D_2$/30 h, then $N_2$/70 h), and the solvent was then removed under reduced pressure. The dark brown solid was extracted with pentane (3 × 50 mL) and filtered, and the filtrate was concentrated to *ca.* 40 mL. Slow cooling of this solution to −80 °C yielded the product as a dark brown solid (0.570 g, 60%), shown to be fully deuterated **1**-$d_2$ by $^1H$ and $^{31}P\{^1H\}$ NMR spectroscopy.

**(dtbpe)PtD$_2$ (6-$d_2$).** A mixture of (dtbpe)$PtCl_2$ (0.50 g, 0.86 mmol) and Na/Hg (0.8%, 50 g) in THF (150 mL) was stirred under $D_2$ (1 atm) at room temperature for 15 h. The mixture was allowed to settle for 4 h and filtered, and the solvent was removed from the filtrate under reduced pressure. A $^1H$ NMR spectrum at this point showed that the crude product was an isotopic mixture of the dideuteride, hydridodeuteride, and dihydride complexes. The dark brown solid was dissolved in toluene (40 mL) and stirred at room temperature under $D_2$ (1 atm) for 90 h. The head space above the solution was then evacuated and refilled with $D_2$ to a pressure of 1 atm, and the solution was stirred for an additional 48 h. The solution was filtered, and the filtrate was concentrated to *ca.* 20 mL. Slow cooling of this solution to −80 °C yielded the product as a beige solid (0.33 g, 74%).

**[(dcype)$_2$Pt$_2$H$_3$][OH].** To a benzene solution (0.5 mL) of **1** (15 mg) was added 2 drops of water, and the mixture was stirred for several minutes. The solvent was removed under reduced pressure, and the pale yellow solid residue was extracted into $CDCl_3$ and placed in an NMR tube. $^1H$ NMR ($CDCl_3$): δ 1.60 (m, 96H), −2.81 (q of q, 3H, $^1J_{PtH}$ = 480 Hz, $^2J_{PH}$ = 39 Hz) ppm. $^{31}P\{^1H\}$ NMR, see Table 7.

**Crystal Structure Determinations of 1 and 3.** Light brown crystals of **1** were obtained from slow cooling of a hexane solution to −40 °C; dark orange crystals of **3** were obtained from slow cooling of a toluene solution to −40 °C. Crystal data and numerical details of the structure determinations are given in Table 3. The crystals were placed in Paratone N oil, mounted on the end of a cut quartz capillary tube, and placed under a flow of cold nitrogen on an Enraf-Nonius CAD4 diffractometer. Intensities were collected with graphite-monochromatized Mo Kα (λ = 0.710 73 Å) radiation using the $\phi-2\phi$ scan technique. Lattice parameters were determined using automatic peak search and indexing procedures. Intensity standards were measured every hour of data collection.

The raw intensity data were converted to structure factor amplitudes and their estimated standard deviations by correction for scan speed, background, and Lorentz and polarization effects. Corrections for crystal decomposition were performed for both data sets. An empirical absorption correction was applied to the data for **1**, after a full isotropic refinement, using the program DIFABS;[22] an empirical correction based on the observed variation in the azimuthal scan data was applied to **3**. The structures were solved by Patterson techniques and refined using standard least-squares and Fourier technique. The secondary extinction coefficient was refined for both data sets, giving final values of 4.28 × $10^{-8}$ for **1** (12% maximum correction on *F*) and 2.01 × $10^{-7}$ for **3** (19% maximum correction on F). Near the end of the refinement cycle, one reflection was rejected from the data set for **1** as a result of an anomalously high $w(\Delta)^2$ value.

For **1**, the hydrogen atoms were placed in idealized positions and included in the structure factor calculations but not refined. All hydrogen atoms were given isotropic thermal parameters of 1.3($B_{iso}$) of the atom to which they were bonded. As the quality of the data was not sufficient, no hydrogen atoms were added to the model for **3**.

On the basis of a difference Fourier map of the heavy atom isotropic model for **3**, five of the eight *tert*-butyl groups of the two phosphine ligands were found to be rotationally disordered (*i.e.*, positive difference peaks were located between the methyl groups of the disordered *tert*-butyl groups). This disorder was modeled by assigning two different carbon atoms to each disordered methyl group, with the multiplicity of each atom assigned on the basis of the intensity ratio of difference peaks (the total multiplicity of the two atoms summing to one). The methyl group of the toluene molecule was also found to be disordered; again a similar modeling technique was used, and two methyl carbons were assigned (on adjacent ring carbons), with the total multiplicity summing to one. All of the heavy atoms were then refined anisotropically, except for the disordered methyl groups of the *tert*-butyl groups

(22) Walker, N.; Stuart, D. *Acta Crystallogr.* **1983**, *A39*, 158.

and also the carbon atoms of the entire toluene molecule (giving a toluene of 33 anisotropic heavy atoms and 26 isotropic heavy atoms in the final model).

The least-squares program minimized the expression, $\sum w(|F_o| - |F_c|)^2$, where $w$ is the weight of a given observation. A value of 0.04 for the $p$ factor was used for both data sets to reduce the weight of intense reflections in the refinements. The analytical forms of the scattering factor tables for the neutral atoms were used, and all non-hydrogen scattering factors were corrected for both real and imaginary components of anomalous dispersion.

**Acknowledgment.** This work was supported by the Director, Office of Energy Research, Office of Basic Energy Sciences, Chemical Sciences Division of the U.S. Department of Energy under Contract No. DE-AC03-76F00098. We thank the National Science Foundation for a predoctoral fellowship to D.J.S., Dr. F. J. Hollander for helpful advice concerning X-ray crystallography, and Dr. Graham Ball for helpful discussions and for help with the 2-D NMR spectra.

**Supplementary Material Available:** Complete tables of bond lengths and angles, anisotropic thermal parameters, hydrogen atom positional parameters (for **1**), root mean-squared amplitudes of thermal vibration, an ORTEP diagram showing all of the disorder in **3**, NMR spectra (a) $^{195}$Pt INEPT spectrum of **1** (85.6 MHz, 25 °C, toluene-$d_3$), (b) $^1$H/$^{31}$P{$^1$H} HMQC spectrum of **1** (300 MHz, −90 °C, toluene-$d_8$), (c) $^1$H/$^{31}$P{$^1$H} HMQC spectrum of the "mixed dimer sample", containing **1**, **2**, and [(dcype)Pt(H)Pt(H)(dippe)] (400 MHz, 25 °C, THF-$d_8$), (d) simulated $^{31}$P{$^1$H} spectrum of **1** at −90 °C (Figure 6a), using the coupling constant values given in the text, including the subspectra for the Pt/Pt, Pt/$^{195}$Pt, and $^{195}$Pt/$^{1}$19$^{5}$Pt isotopomers, and (e) experimental $^1$H/$^{195}$Pt HMQC spectrum of **1** (300 MHz, −90 °C, toluene-$d_8$), with the simulated $^{195}$Pt{$^1$H} spectrum, using the coupling constant values given in the text, including the subspectra for the Pt/$^{195}$Pt and $^{195}$Pt/$^{195}$Pt isotopomers (40 pages); tables of observed and calculated structure factors (77 pages). This material is contained in many libraries on microfiche, immediately follows this article in the microfilm version of the journal, can be ordered from the ACS, and can be downloaded from the Internet; see any current masthead page for ordering information and Internet access instructions.

JA942502G